



DOI: 10.34910/MCE.102.10

Heat release and thermal conductivity of expanded-clay concrete for 3D printer

K. Usanova^{a*}, Yu.G. Barabanshchikov^a, L. Pakrastins^b, S.V. Akimov^a, S.V. Belyaeva^a

^a Peter the Great St. Petersburg Polytechnic University, St. Petersburg, Russia

^b Riga Technical University, Riga, Latvia

*E-mail: plml@mail.ru

Keywords: claydite concrete, expanded-clay concrete, cement, superplasticizer, heat release, heat of hydration, thermal conductivity, permeability of heat, thermal transmittance, 3D printer, regression analysis, furnace slag, silica fume

Abstract. The subject of research is expanded-clay concrete with additives of ground granulated blast-furnace slag, silica fume, superplasticizer admixture and air-entraining admixture for 3D printing. The heat release of concrete and thermal conductivity of concrete are investigated depending on the concrete composition (cement, water cement ratio, expanded-clay), additives (slag, silica fume) and admixtures (superplasticizer, air-entraining agent). The thermal conductivity of concrete depends primarily on the expanded clay gravel content and depends less on the cement content. If both factors increase, the thermal conductivity decreases. This is due to the replacement of dense sand grains with a more porous cement paste. The influence of air-entraining admixture on the thermal conductivity of expanded-clay concrete was not detected due to the high scattering of the experimental points. It was confirmed that the cement content and water cement ratio have an impact on the integral value of the heat release per unit mass of cement ($q = Q/C$). This value decreases with increasing cement content. The reason for this is that the total heat generated by concrete Q , with constant W/C and other equal conditions, increases linearly with increasing the cement content. The air-entraining admixture increases the heat generation by concrete. This is due to the chemical interaction between the admixture and cement hydration products with the formation of thermodynamically more stable compounds.

1. Introduction

The technology of 3D printing is gradually becoming an integral part of construction industry. Using construction 3D printers automates the manufacturing process of building products and the construction.

3D printers create of an object by adding material to the object layer by layer. The physical object is usually based on a digital 3D model [1–2]. In the construction industry, 3D printing can be used over a wide range: from the creation of hardscape elements [3] to the creation of large structures such as walls and domes [4].

3D printing in construction industry makes it possible to realize not only simple rectangular buildings, but also structures more complex in their geometry [5]. In addition, the positive effects are the opportunity to reduce the cost of the created objects, increase the accuracy of their manufacture and reduce the construction period [6], [7].

The properties of concrete mix for 3D printing technology makes many demands [8]. The mixture must have a certain viscosity and moldability to maintain the required shape during printing. In addition, the mixture must have workability for extrusion [9]. It should also be fast setting, so as not to lose shape without formwork [10–11]. If it is necessary for concrete to have greater strength, steel reinforcement, fiber or glass-fiber are added to the mixture [12–16]. Possible flexural strength is up to 30 MPa and compressive strength is up to 80 MPa in the case of using carbon, glass and basalt fibers with a size of 3–6 mm [17–18]. It is possible to use lightweight steel concrete structures consisting of monolithic concrete, profiled steel and fiber-cement sheets [19–20].

Usanova, K., Barabanshchikov, Yu.G., Pakrastins, L., Akimov, S.V., Belyaeva, S.V. Heat release and thermal conductivity of expanded-clay concrete for 3D printer. Magazine of Civil Engineering. 2021. 102(2). Article No. 10210. DOI: 10.34910/MCE.102.10



This work is licensed under a [CC BY-NC 4.0](https://creativecommons.org/licenses/by-nc/4.0/)

Other additives may be included in the mixture to improve certain characteristics of the concrete mix or concrete structures [21].

Experimental studies [22–23] showed that the addition of silica and nanoclay improved the formability of the fresh printing mixture, while a slight improvement was observed as a result of the addition of polypropylene fiber [24]. It is possible to use cement with clay soil and additives. The test results [25] shows the possibility of replacing cement paste with clay soil up to 25 % which leads to a reduction in the cost and an increase in printability with a slight decrease in the strength of the obtained material to 7 %. Other mineral admixture (fly ash, blast furnace slag, limestone, silica, silica fume, nanosilica, granite, perlite, vermiculite, etc.) also improved the properties of concrete [26–28].

The study [29] investigated adhesion between the layers of 3D printed concrete. It was found that the adhesion between the layers decreased with increasing time interval between lay-up. The interlayer bonds can be strengthened with cement paste at the interface [30]. This solution minimized voids and increased the adhesion area.

Good extrudability and buildability were achieved when the yield strength of the material was in the range of 1.5–2.5 kPa [31]. The material did not have enough strength for maintain shape if the yield strength was below this range. Nevertheless, the material extrudability was difficult if the yield strength was above this range.

For additive technologies due to the absence of form work, the rheological properties of the concrete mixture and green strength are also significant [9, 32]. As for example, the green strength can be up to 9.5 kPa in 30 min after mortar extrusion and up to 45 kPa in 150 min after mortar extrusion [32]. In this paper, rheological properties and green strength are not considered.

In addition to the above concrete properties, which play an important role for 3D printing, it is the heat release of concrete [33]. Cracks appear in hardening concrete because of the heat of hydration of cement. These cracks are caused by uneven and moderate temperature deformations [34], [35]. There are different technical solutions for controlling the thermal conditions of hardening concrete and reducing temperature differences [36], [37], [38].

Another important property of any types of concrete is its thermal conductivity [39]. The thermal conductivity significantly affects the thermotechnical characteristics of the building and its energy performance [40–41].

In study [42], concrete containing cement, fly ash and hydrophobic aerogel granules was investigated. This type of composite could be used as 3D printing of wall elements with low thermal conductivity.

Another way to reduce the thermal conductivity was to use the extrudable foamed concrete [43–44]. Study [43] showed that the obtained green and early age strength made this material potentially suitable for 3D printing. Relatively high compressive strengths of this concrete was above 10 MPa [44]. Therefore, it fulfilled the requirements for building materials used for load-bearing wall elements in multi-story houses. This type of concrete was suitable for 3D-printing applications, while fulfilling both load-carrying and insulating functions. Besides the foamed concrete could be used foamed fly ash-based geopolymer matrices. This material for 3D printing was investigated in [45].

Large scale building elements could be made on 3D printer by depositing fresh wood chip concrete [46].

Fiber-reinforced concrete was investigated in [47] to optimize the mechanical and heat transfer characteristics of building components. Structures made of this type of concrete showed less thermal conductivity compared to reinforced concrete.

However, the heat release of concrete and the thermal conductivity of concrete has not yet been purposefully investigated for construction 3D printing. Which makes this research relevant.

The subject of research is expanded-clay concrete with additives of ground granulated blast-furnace slag, silica fume, superplasticizer admixture and air-entraining admixture for 3D printing.

The objectives of the work is analysis of expanded-clay concrete composition influence on the heat release and the thermal conductivity of concrete.

2. Materials and Methods

2.1. Materials

The Fly ash aggregate was tested in Peter the Great St. Petersburg Polytechnic University (Russia).

Consistency of experimental mixtures was not tested for 3D printing. The rheological parameters for suitability can be achieved using admixtures after selecting a mixture according to the criteria of heat release and thermal conductivity.

Concrete mixture consisted of:

1. Portland cement PC 500-D0-N produced by OJSC MORDOVCEMENT (Mordovia, Russia). Fineness of the cement is 97.1 %. Mineralogical composition of the cement are presented in Table 1.

Table 1. Mineralogical composition of the cement [%].

C ₃ S	C ₂ S	C ₃ A	C ₄ AF
60.8	16.6	5.8	12.8

2. Natural sand. The sand has fineness modulus from 2 to 2.5.

3. Expanded clay gravel produced by OOO SUOR (Novocheboksarsk, Russia). Size fraction is 0–20 mm, bulk density is 800 kg/m³ and cylinder strength is from 5.5 to 6.5 MPa.

4. Silica fume MKU-85 produced by Yurga division of Kuznetskie Ferrosplavy (Yurga, Russia). Specific surface area is 15 m²/g. Content of SiO₂ is 91.2 %.

5. Ground granulated blast furnace slag produced by PJSC Mechel (Russia). Chemical composition of the slag is presented in Table 2.

Table 2. Chemical composition of the ground granulated blast furnace slag.

S	K	SiO ₂	CaO	MnO	Al ₂ O ₃	MgO	TiO ₂	FeO
0.710	1.54	38.90	40.50	0.57	10.50	7.50	0.73	0.63

6. Superplasticizer Sika ViscoCrete E78 RC/A on the base of polycarboxylate.

7. Air-entraining admixture Sika AER 200-C on the base of synthetic surface-active agent.

2.2. Thermal conductivity measurement

The thermal conductivity λ was determined by thermal conductivity meter ITP-MG4 “250” according to Russian State Standard GOST 7076-99 “Building materials and products. Method of determination of steady-state thermal conductivity and thermal resistance”. Samples in the form of plates were made with dimensions of 250×250×30 mm. Form removal was carried out 2 days after the manufacture of the samples. After that, the samples were stored under normal conditions at a temperature of 20 ± 2 °C and a relative air humidity of at least 96 %. After 28 days, the samples were removed from the moisture chamber and dried to constant weight. The test results are presented in Table 3.

2.3. Heat release measurement

Heat release Q was determined according to EN 196-9:2010. The heat release of concrete was determined by the thermos method at an initial temperature of 20 °C. After that, the heat release of concrete was recalculated to the isothermal hardening mode at a temperature of 20 °C.

In accordance with hypothesis [48] the ratio of the heat release rates and corresponding terms τ_2 and τ_1 remains constant at moments of equal heat release at $Q_1 = Q_2$:

$$\frac{(\partial Q / \partial \tau)_1}{(\partial Q / \partial \tau)_2} = \frac{\tau_2}{\tau_1} = f_t = \text{const} \quad (1)$$

The temperature function f_t was calculated by the formula:

$$f_t = 2^{\frac{t_1 - t_2}{\varepsilon}}, \quad (2)$$

where ε is the characteristically temperature difference. If $t_1 - t_2 = \varepsilon$, when $f_t = 2$. This means if the temperature rises by ε degrees, the rate of heat release will double.

Three identical samples of each concrete mix were tested. The readings of the temperature sensors were recorded by the data logger every 30 minutes. Heat release per unit mass of cement $q = Q/C$ in tested mixes was characterized by two parameters of the I.D. Zaporozhets's equation (3): $q_{\max} = Q_{\max}/C$, kJ/kg and A_{20} , d⁻¹. The parameter m was accepted constant and equal to 2.2 [49].

$$Q = Q_{\max} \left[1 - (1 + A_t \tau)^{-\frac{1}{m-1}} \right], \quad (3)$$

where A_t is the heat release rate coefficient that characterizes the heat release rate at a given constant temperature t (in this case $t = 20$ °C and $A_t = A_{20}$); m is the order of the cement hydration reaction. The order of the cement hydration reaction for portland cement is between 2 and 2.3.

The values of q_{\max} and A_{20} were determined by experimental data.

3. Results and Discussion

3.1. Experimental data of heat release and thermal conductivity

The heat release data and the thermal conductivity data of expanded-clay concrete are presented in Table 3.

Table 3. Mixture proportions, the heat release and the thermal conductivity of expanded-clay concrete.

Cement (C) [kg/m ³]	W/C	Expanded clay gravel [kg/m ³]	Sika VC E78 [kg/m ³]	Sika AER 200-C [kg/m ³]	Silica fume [kg/m ³]	Slag [kg/m ³]	λ [W/(m·°C)]	q_{\max} [kJ/kg]	A_{20} [d ⁻¹]
X_1	X_2	X_3	X_4	X_5	X_6	X_7	Y_1	Y_2	Y_3
375	0.445	0	4.5	1	0	60	1.352	400	1.45
375	0.45	0	5.25	0	0	60	1.378	380	1.65
430	0.43	130	4.5	1.45	43	70	1.215	392	1.45
435	0.425	276	4.34	1.53	44	70	1.071	420	1.23
440	0.461	347	3.96	1.38	44	70	0.983	423	0.8
450	0.438	115	4.32	1	45	80	1.191	393	1.25
450	0.511	520	4.05	1	45	70	0.791	395	0.9
460	0.374	267	4.15	1	46	80	1.018	360	2
460	0.439	185	4.4	0.8	46	70	1.184	420	1.25
465	0.35	545	3.75	0.75	40	0	0.751	335	0.9
465	0.443	295	4.9	1.4	46	70	0.994	430	1.15
465	0.35	545	3.75	0.75	40	0	0.855	330	1.1
470	0.483	270	4.23	1.4	47	69	0.954	420	1.05
475	0.309	602	5	0.55	44	0	0.842	355	1.5
475	0.314	502	4.5	0	44	0	0.788	350	1.7
475	0.34	0	3.7	0	45	0	0.918	320	1.33
475	0.319	502	5	0	44	0	0.848	360	1.3
475	0.318	602	5.5	0.55	44	0	0.885	360	1.3
475	0.34	560	3.7	0	45	0	0.901	317	1.4
480	0.429	430	4.35	0.85	50	70	0.94	330	0.86
485	0.404	530	6	0	45	110	0.867	380	2.5
490	0.414	351	5.8	1	48	68	0.878	370	1.35
520	0.296	486	7.6	1.25	50	60	0.83	345	1.1
520	0.337	504	6.7	0	50	100	0.858	325	3.3
520	0.379	400	7.5	0	45	60	0.906	350	1.3
520	0.404	556	6.4	0	50	50	0.86	330	2.8
520	0.41	428	4.9	1.5	50	70	0.791	358	1.55
550	0.351	512	6.25	0	50	50	0.77	310	1.05

3.2. Thermal conductivity dependence on concrete composition

The influence of independent composition parameters ($X_1 \dots X_7$) on the thermal conductivity parameters (Y_1) is determined by multivariate analysis based on linear regression.

Linear regression $Y_1 = f(X_1 \dots X_7)$ is appropriate according to the F-test, which is $4.32E-12$ with a statistical value of 60.7. A determination coefficient R^2 is 0.9550. The regression coefficients and their significance are given in Table. 4.

Table 4. Parameters of linear regression for the thermal conductivity dependence on concrete composition.

Variables	coefficients	Standard error	t-statistics	P-value	Limits of confidence 95 %	
					Upper	Lower
X_1	-0.00176	0.000610	-2.88	0.00916	-0.00303	-0.000487
X_2	-0.154	0.270	-0.569	0.576	-0.717	0.410
X_3	-7.79E-04	6.55E-05	-11.9	1.59E-10	-9.15E-04	-6.42E-04
X_4	0.0125	0.0148	0.847	0.407	-0.0183	0.0433
X_5	-0.0448	0.0198	-2.26	0.0349	-0.0861	-0.00352
X_6	0.00126	0.00164	0.766	0.453	-0.00217	0.00468
X_7	0.000546	0.000472	1.16	0.261	-0.000439	0.00153
Y_1 interaction	2.02	0.239	8.44	5.02E-08	1.52	2.52

Size of a region meets the condition $P < 0.05$ for three of seven factors. These factors are X_1 (cement content), X_3 (expanded-clay gravel content) and X_5 (air-entraining admixture content). Moreover, all three coefficients are negative, that is, an increase in the content of each of these components reduces the value of thermal conductivity of concrete. However, the results of dual regression analysis shows that coefficient of X_5 is positive, which contradicts the physical meaning, and the coefficient of determination is very small, $R^2 = 0.0292$. Linear regression plots for significant factors X_1 and X_3 are shown in Fig. 1.

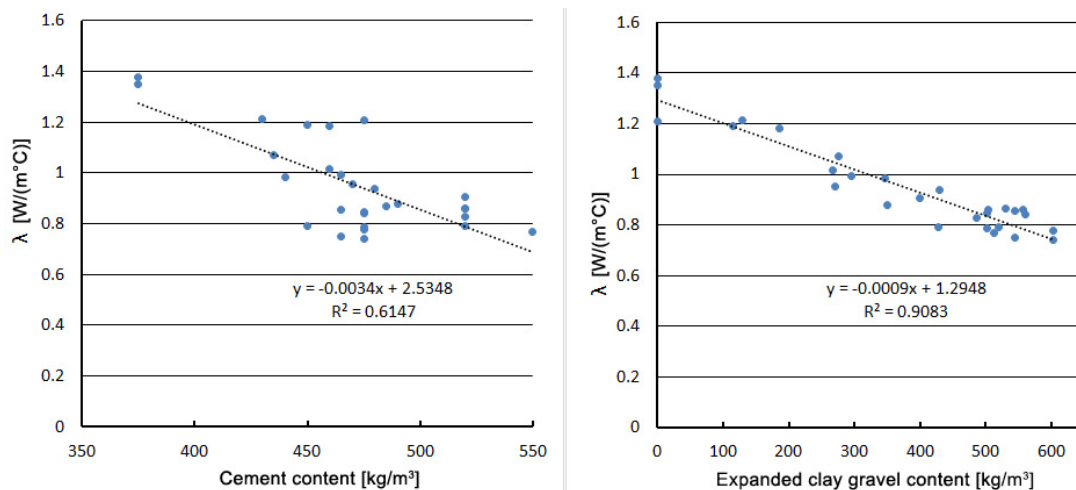


Figure 1. Dual regression plots for the dependence of thermal conductivity versus cement content, and expanded clay gravel content.

3.3. Heat release dependence on concrete composition

The influence of independent composition parameters ($X_1 \dots X_7$) on the heat release parameters (Y_2 and Y_3) was determined by multivariate analysis based on linear regression. Importance factors are presented in Table 5.

Table 5. Linear hypothesis factors of the multifactorial regression.

Regression	F-statistics	F-value	R^2
$q_{max} = Y_2 = f(X_1 \dots X_7)$	9.70	2.95E-05	0.7725
$A_{20} = Y_3 = f(X_1 \dots X_7)$	3.63	0.0109	0.5598

Linear regression graphs for the most significant factors X_1 , X_2 , and X_5 of the response function $Y_2 = q_{max}$ are shown in Fig. 2.

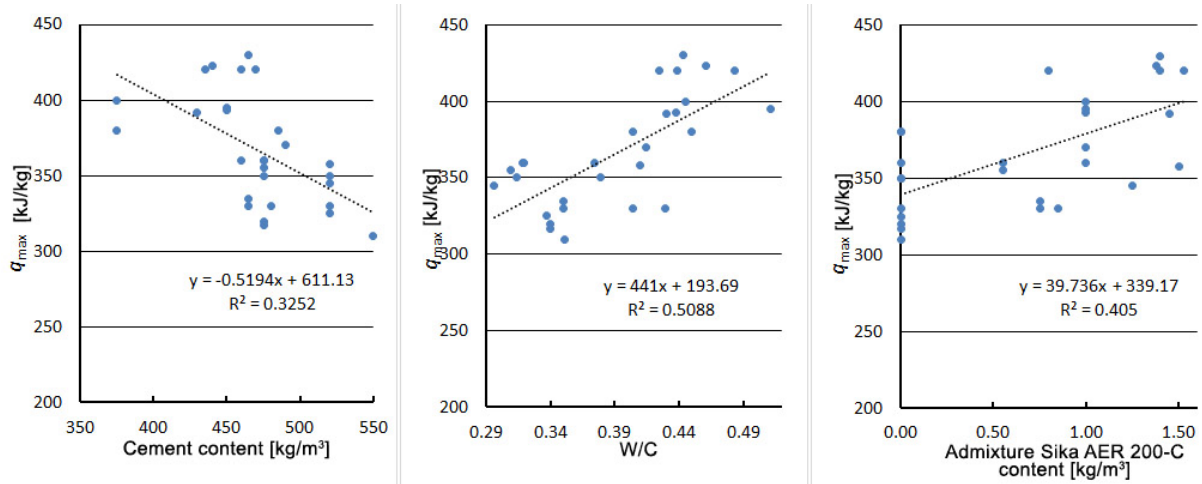


Figure 2. Dual regression plots for the dependence of q_{max} versus cement content, water-cement ratio and admixture Sika AER 200-C content.

Function $Y_3 = A_{20}$ has very low coefficients of determination for the dual regression and represents hundredths and thousandths of a unit.

3.4. Correlation between the concrete parameters

The results of regression analysis on the influence of seven factors on the thermal conductivity (Y_1) shows that only two factors have significant statistical value. The thermal conductivity decreases with increasing the expanded clay gravel content (factor X_3), which is characterized by a relatively small scattering of points and a high coefficient of determination of $R^2 = 0.9083$. The influence of another significant factor – cement content (X_1) – is difficult to explain. If the cement content increases, the thermal conductivity decreases. Two more dual regressions of dependencies could explain this fact. They are concrete density versus cement content and thermal conductivity versus concrete density (Fig. 3).

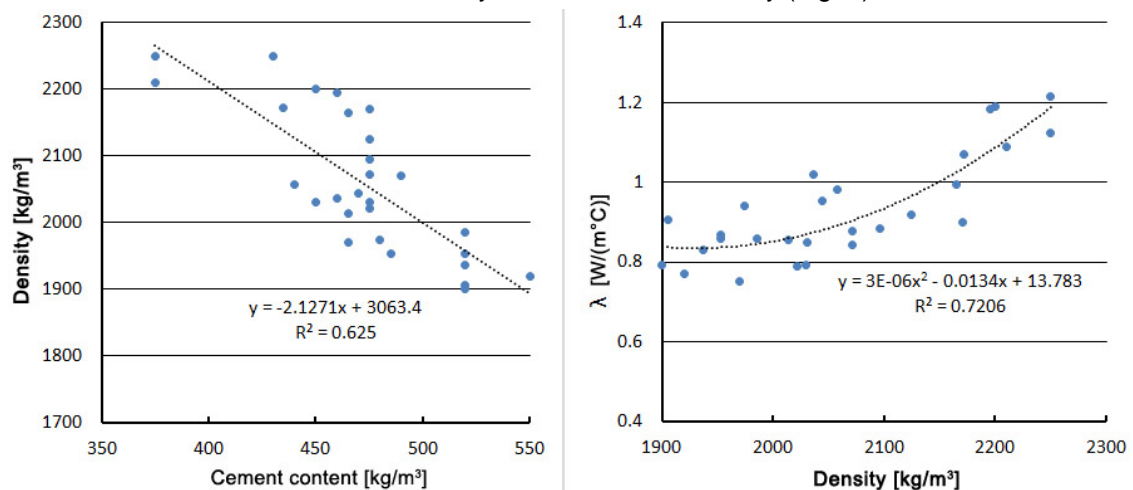


Figure 3. Dual regressions of dependencies: concrete density versus cement content and thermal conductivity versus concrete density.

As shown in Fig. 3, the effect of cement content (factor X_1) on the thermal conductivity (Y_1) is associated with a decrease in the concrete density. Authors assume that this is the result of replacement of fine aggregate with a more porous cement paste. In this case, the usual correlation between λ and the concrete density is satisfactorily described by a second degree polynomial with a determination coefficient of $R^2 = 0.721$.

As a regression analysis has shown, the total integral value of the heat release per unit mass of cement q_{max} (Y_2) depends on three factors: the cement content (X_1), the water cement ratio (X_2) and the admixture Sika AER 200-C content (X_5). Fig. 2 shows a significant scattering of experimental points, but a certain tendency is observed. The decrease in the heat release per unit mass of cement $q = Q/C$ with an increase in cement content is a well-known position. The heat Q produced by concrete, with constant W/C and other

equal conditions, increases linearly with an increase in the cement content C [50], [51]. This explains the law of mass action from chemical kinetics.

4. Conclusions

A multivariate analysis of experimental data on the influence of seven factors of concrete mixture (cement, water cement ratio, expanded clay, ground granulated blast-furnace slag, silica fume, superplasticizer, air-entraining admixture) on the thermal conductivity and the heat release of concrete was carried out. The results obtained lead to the following conclusions:

1. The thermal conductivity of concrete depends primarily on the expanded clay gravel content and depends less on the cement content. If both factors increase, the thermal conductivity decreases. This is due to the replacement of dense sand grains with a more porous cement paste. The influence of air-entraining admixture on the thermal conductivity of expanded-clay concrete was not detected due to the high scattering of the experimental points.
2. The cement content and water cement ratio impact on the integral value of the heat release per unit mass of cement. This value $q = Q/C$ decreases with increasing cement content. The reason for this is that the heat Q generated by concrete, with constant W/C and other equal conditions, increases linearly with increasing the cement content C . W/C has a positive effect on the heat release of concrete. This explains the law of mass action from chemical kinetics.
3. The influence of these seven factors on the rate of heat release, and, consequently, on the hydration of cement has not been established.

Further research on this topic may be experimental studies of cold-bonded fly ash aggregate concrete for 3D printer. Fly ash can be used as an additive in the mix [52] or as a large aggregate [53]. If presoaked aggregate is added to the concrete mix, this will create "internal curing" for the concrete and reduce cracks caused by the heat release [54].

5. Acknowledgements

The research is funded by the Ministry of Science and Higher Education of the Russian Federation as part of World-class Research Center program: Advanced Digital Technologies (contract No. 075-15-2020-934 dated 17.11.2020).

References

1. Ngo, T.D., Kashani, A., Imbalzano, G., Nguyen, K.T.Q., Hui, D. Additive manufacturing (3D printing): A review of materials, methods, applications and challenges. *Compos. Part B Eng.* 2018. 143. Pp. 172–196. DOI: 10.1016/j.compo-sitesb.2018.02.012.
2. Vatin, N.I., Usanova, K.Y. BIM end-to-end training: From school to graduate school. *Adv. Trends Eng. Sci. Technol. III- Proc. 3rd Int. Conf. Eng. Sci. Technol. ESaT 2018.* 2019. Pp. 651–656. DOI: 10.1201/9780429021596-102
3. Lowke, D., Dini, E., Perrot, A., Weger, D., Gehlen, C., Dillenburger, B. Particle-bed 3D printing in concrete construction – Possibilities and challenges. *Cem. Concr. Res.* 2018. 112. Pp. 50–65. DOI: 10.1016/j.cemconres.2018.05.018.
4. Lim, S., Buswell, R.A., Valentine, P.J., Piker, D., Austin, S.A., De Kestelier, X. Modelling curved-layered printing paths for fabricating large-scale construction components. *Addit. Manuf.* 2016. 12. Pp. 216–230. DOI: 10.1016/j.addma.2016.06.004
5. Gosselin, C., Duballet, R., Roux, P., Gaudillière, N., Dirrenberger, J., Morel, P. Large-scale 3D printing of ultra-high performance concrete – a new processing route for architects and builders. *Mater. Des.* 2016. 100. Pp. 102–109. DOI: 10.1016/j.matdes.2016.03.097
6. Akulova, I., Slavcheva, G. Methodical Approach to Calculation of the Maintenance Cost for 3D Built Printing Equipment. *IOP Conf. Ser. Mater. Sci. Eng.* 2020. 753. DOI: 10.1088/1757-899X/753/5/052056
7. Tay, Y.W.D., Panda, B., Paul, S.C., Noor Mohamed, N.A., Tan, M.J., Leong, K.F. 3D printing trends in building and construction industry: a review. *Virtual Phys. Prototyp.* 2017. 12. Pp. 261–276. DOI: 10.1080/17452759.2017.1326724
8. Elistratkin, M.Y., Lesovik, V.S., Alfimova, N.I., Shurakov, I.M. On the question of mix composition selection for construction 3D printing. *Mater. Sci. Forum.* 945 MSF. 2018. Pp. 218–225. DOI: 10.4028/www.scientific.net/MSF.945.218
9. Slavcheva, G.S., Artamonova, O.V. Rheological behavior and mix design for 3D printable cement paste. *Key Eng. Mater.* 799 KEM. 2019. Pp. 282–287. DOI: 10.4028/www.scientific.net/KEM.799.282
10. Bos, F., Wolfs, R., Ahmed, Z., Salet, T. Additive manufacturing of concrete in construction: potentials and challenges of 3D concrete printing. *Virtual Phys. Prototyp.* 2016. 11. Pp. 209–225. DOI: 10.1080/17452759.2016.1209867
11. De Schutter, G., Lesage, K., Mechtcherine, V., Nerella, V.N., Habert, G., Agusti-Juan, I. Vision of 3D printing with concrete – Technical, economic and environmental potentials. *Cem. Concr. Res.* 2018. 112. Pp. 25–36. DOI: 10.1016/j.cem-conres.2018.06.001
12. Paul, S.C., van Zijl, G.P.A.G., Gibson, I. A review of 3D concrete printing systems and materials properties: current status and future research prospects. *Rapid Prototyp. J.* 2018. 24. Pp. 784–798. DOI: 10.1108/RPJ-09-2016-0154
13. Bos, F.P., Ahmed, Z.Y., Wolfs, R.J.M., Salet, T.A.M. 3D printing concrete with reinforcement. *High Tech Concr. Where Technol. Eng. Meet – Proc. 2017 fib Symp.* 2017. Pp. 2484–2493. DOI: 10.1007/978-3-319-59471-2_283
14. Klyuev, S.V., Klyuev, A.V., Shorstova, E.S. Fiber concrete for 3-D additive technologies. *Mater. Sci. Forum.* 2019. 974. Pp. 367–372. DOI: 10.4028/www.scientific.net/MSF.974.367
15. Klyuev, S.V., Klyuev, A.V., Vatin, N.I. Fiber concrete for the construction industry. *Magazine of Civil Engineering.* 2018. 84. Pp. 41–47. DOI: 10.18720/MCE.84.4

16. Murali, G., Fediuk, R. A Taguchi approach for study on impact response of ultra-high-performance polypropylene fibrous cementitious composite. *J. Build. Eng.* 2020. 30. DOI: 10.1016/j.jobbe.2020.101301
17. Hambach, M., Volkmer, D. Properties of 3D-printed fiber-reinforced Portland cement paste. *Cem. Concr. Compos.* 2017. DOI: 10.1016/j.cemconcomp.2017.02.001
18. Ibragimov, R.A., Izotov, V.S. Effect of carbon nanotubes on the structure and properties of cement composites. *Inorg. Mater.* 2015. 51. Pp. 834–839. DOI: 10.1134/S0020168515080087
19. Rybakov, V., Seliverstov, A., Petrov, D., Smirnov, A., Volkova, A. Lightweight steel concrete structures slab panels load-bearing capacity. *MATEC Web Conf.* 2018. 245. DOI: 10.1051/mateconf/201824508008
20. Rybakov, V.A., Ananeva, I.A., Pichugin, E.D., Garifullin, M. Heat protective properties of enclosure structure from thin-wall profiles with foamed concrete. *Magazine of Civil Engineering.* 2020. 94(2). Pp. 11–20. DOI: 10.18720/MCE.94.2
21. Soltan, D.G., Li, V.C. A self-reinforced cementitious composite for building-scale 3D printing. *Cem. Concr. Compos.* 2018. DOI: 10.1016/j.cemconcomp.2018.03.017
22. Zareiyan, B., Khoshnevis, B. Effects of interlocking on interlayer adhesion and strength of structures in 3D printing of concrete. *Autom. Constr.* 2017. 83. Pp. 212–221. DOI: 10.1016/j.autcon.2017.08.019
23. Zareiyan, B., Khoshnevis, B. Effects of mixture ingredients on interlayer adhesion of concrete in Contour Crafting. *Rapid Prototyp. J.* 2018. 24. Pp. 584–592. DOI: 10.1108/RPJ-02-2017-0029
24. Kazemian, A., Yuan, X., Cochran, E., Khoshnevis, B. Cementitious materials for construction-scale 3D printing: Laboratory testing of fresh printing mixture. *Constr. Build. Mater.* 2017. DOI: 10.1016/j.conbuildmat.2017.04.015
25. Iubin, P., Zakrevskaya, L. Soil-concrete for use in the 3D printers in the construction of buildings and structures. In: *MATEC Web of Conferences.* EDP Sciences. 2018. DOI: 10.1051/mateconf/201824503002
26. Klyuev, S.V., Klyuev, A.V., Shorstova, E.S. The micro silicon additive effects on the fine-grassed concrete properties for 3-D additive technologies. *Mater. Sci. Forum.* 2019. 974. Pp. 131–135. DOI: 10.4028/www.scientific.net/MSF.974.131
27. Ma, G., Wang, L. A critical review of preparation design and workability measurement of concrete material for largescale 3D printing. *Front. Struct. Civ. Eng.* 2018. 12. Pp. 382–400. DOI: 10.1007/s11709-017-0430-x
28. Rybakov, V., Seliverstov, A., Petrov, D., Smirnov, A., Volkova, A. Strength characteristics of foam concrete samples with various additives. *MATEC Web Conf.* 2018. 245. DOI: 10.1051/mateconf/201824503015
29. Wolfs, R.J.M., Bos, F.P., Salet, T.A.M. Hardened properties of 3D printed concrete: The influence of process parameters on interlayer adhesion. *Cem. Concr. Res.* 2019. 119. Pp. 132–140. DOI: 10.1016/j.cemconres.2019.02.017
30. Marchment, T., Sanjayan, J., Xia, M. Method of enhancing interlayer bond strength in construction scale 3D printing with mortar by effective bond area amplification. *Mater. Des.* 2019. 169. DOI: 10.1016/j.matdes.2019.107684
31. Rahul, A.V., Santhanam, M., Meena, H., Ghani, Z. 3D printable concrete: Mixture design and test methods. *Cem. Concr. Compos.* 2019. 97. Pp. 13–23. DOI: 10.1016/j.cemconcomp.2018.12.014
32. Ding, T., Xiao, J., Qin, F., Duan, Z. Mechanical behavior of 3D printed mortar with recycled sand at early ages. *Constr. Build. Mater.* 2020. 248. DOI: 10.1016/j.conbuildmat.2020.118654
33. Shanahan, N., Tran, V., Zayed, A. Heat of hydration prediction for blended cements. *J. Therm. Anal. Calorim.* 2017. 128. Pp. 1279–1291. DOI: 10.1007/s10973-016-6059-5
34. Klemczak, B., Batog, M., Pilch, M., Zmij, A. Analysis of Cracking Risk in Early Age Mass Concrete with Different Aggregate Types. *Procedia Eng.* 2017. 193. Pp. 234–241. DOI: 10.1016/j.proeng.2017.06.209
35. Shaibakova, A., Semenov, K., Barabanshchikov, Y. Thermal cracking resistance of stacking concrete blocks. *MATEC Web Conf.* 2018. 245. DOI: 10.1051/mateconf/201824508005
36. Singh, P.R., Rai, D.C. Effect of piped water cooling on thermal stress in mass concrete at early ages. *J. Eng. Mech.* 2018. 144. DOI: 10.1061/(ASCE)EM.1943-7889.0001418
37. Azenha, M., Lameiras, R., de Sousa, C., Barros, J. Application of air cooled pipes for reduction of early age cracking risk in a massive RC wall. *Eng. Struct.* 2014. 62–63. Pp. 148–163. DOI: 10.1016/j.engstruct.2014.01.018
38. Seo, T.S., Kim, S.S., Lim, C.K. Experimental study on hydration heat control of mass concrete by vertical pipe cooling method. *J. Asian Archit. Build. Eng.* 2015. 14. Pp. 657–662. DOI: 10.3130/jaabe.14.657
39. Baghban, M.H. Thermal insulating cementitious composite containing aerogel and phosphate-based binder. *IOP Conf. Ser. Mater. Sci. Eng.* 2019. 609. DOI: 10.1088/1757-899X/609/6/062024
40. Gorshkov, A., Vatin, N., Nemova, D., Shabaldin, A., Melnikova, L., Kirill, P. Using life-cycle analysis to assess energy savings delivered by building insulation. *Procedia Eng.* 2015. 117. Pp. 1080–1089. DOI: 10.1016/j.proeng.2015.08.240
41. Gorshkov, A.S., Vatin, N.I., Rymkevich, P.P., Kydrevich, O.O. Payback period of investments in energy saving. *Magazine of Civil Engineering.* 2018. No. 78(2). Pp. 65–75. DOI: 10.18720/MCE.78.5
42. Baghban, M.H., Javadabadi, M.T. Effect of hydrophobic aerogel granules on thermomechanical properties of cementitious composites. *Mater. Sci. Forum.* 971 MSF. 2019. Pp. 114–118. DOI: 10.4028/www.scientific.net/MSF.971.114
43. Falliano, D., Gugliandolo, E., De Domenico, D., Ricciardi, G. Experimental investigation on the mechanical strength and thermal conductivity of extrudable foamed concrete and preliminary views on its potential application in 3D printed multilayer insulating panels. *RILEM Bookseries.* 2019. 19. Pp. 277–286. DOI: 10.1007/978-3-319-99519-9_26
44. Markin, V., Nerella, V.N., Schröfl, C., Guseynova, G., Mechtcherine, V. Material design and performance evaluation of foam concrete for digital fabrication. *Materials (Basel).* 2019. 12. DOI: 10.3390/ma12152433
45. Alghamdi, H., Neithalath, N. Synthesis and characterization of 3D-printable geopolymeric foams for thermally efficient building envelope materials. *Cem. Concr. Compos.* 2019. 104. DOI: 10.1016/j.cemconcomp.2019.103377
46. Henke, K., Talke, D., Winter, S. Additive manufacturing of building elements by extrusion of wood concrete. *WCTE 2016 – World Conf. Timber Eng.* 2016.
47. Vantghem, G., Boel, V., De Corte, W., Steeman, M. Compliance, stress-based and multi-physics topology optimization for 3D-printed concrete structures. In: *RILEM Bookseries.* Pp. 323–332. Springer Netherlands, 2019. DOI: 10.1007/978-3-319-99519-9_30
48. Zaporozhets, I.D., Okorokov, S.D., Pariyskiy, A.A. Heat Liberation by concrete. *Stroyizdat, Moscow (1966).*
49. Makeeva, A., Amelina, A., Semenov, K., Barabanshchikov, Y. Temperature action in analysis of thermal stressed state of massive concrete and reinforced concrete structures. *MATEC Web Conf.* 245. 2018. DOI: 10.1051/mateconf/201824503016

50. Yang, K.H., Moon, G.D., Jeon, Y.S. Implementing ternary supplementary cementing binder for reduction of the heat of hydration of concrete. *J. Clean. Prod.* 2016. 112. Pp. 845–852. DOI: 10.1016/j.jclepro.2015.06.022
51. Bohloli, B., Skjølsvold, O., Justnes, H., Olsson, R., Grøv, E., Aarset, A. Cements for tunnel grouting – Rheology and flow properties tested at different temperatures. *Tunn. Undergr. Sp. Technol.* 2019. 91. DOI: 10.1016/j.tust.2019.103011
52. Fediuk, R.S., Yushin, A.M. The use of fly ash the thermal power plants in the construction. *IOP Conf. Ser. Mater. Sci. Eng.* 2015. 93. DOI: 10.1088/1757-899X/93/1/012070
53. Usanova, K.Y., Barabanshchikov, Y.G., Kostyrya, S.A., Fedorenko, Y.P. Cold-bonded fly ash aggregate as a coarse aggregate of concrete. *Constr. Unique Build. Struct.* 2018. 72. Pp. 1–16.
54. Barabanshchikov, Y., Fedorenko, I., Kostyrya, S., Usanova, K. Cold-Bonded Fly Ash Lightweight Aggregate Concretes with Low Thermal Transmittance: Review. *Adv. Intell. Syst. Comput.* 2019. 983. Pp. 858–866. DOI: 10.1007/978-3-030-19868-8_84

Contacts:

Kseniia Usanova, plml@mail.ru

Yuriy Barabanshchikov, ugb@mail.ru

Leonids Pakrastins, leonids.pakrastins@rtu.lv

Stanislav Akimov, akimov_sv@spbstu.ru

Svetlana Belyaeva, belyaeva_sv@spbstu.ru

© Usanova, K., Barabanshchikov, Yu.G., Pakrastins, L., Akimov, S.V., Belyaeva, S.V., 2021